Neonatal head and torso vibration exposure during inter-hospital transfer

Laurence Blaxter[1], Mildrid Yeo[2], Donal McNally[1], John Crowe[1], Caroline Henry[2], Sarah Hill[2], Neil Mansfield[3], Andrew Leslie[4], Don Sharkey[3,4]

Abstract

Inter-hospital transport of premature infants is increasingly common given the centralisation of neonatal intensive care. However, it is known to be associated with anomalously increased morbidity, most notably brain injury, and with increased mortality from multifactorial causes. Surprisingly, there have been relatively few previous studies investigating the levels of mechanical shock and vibration hazard present during this vehicular transport pathway.

Using a custom inertial datalogger, and analysis software, we quantify vibration and linear head acceleration. Mounting multiple inertial sensing units on the forehead and torso of neonatal patients and a preterm manikin, and on the chassis of transport incubators over the duration of inter-site transfers, we find that the resonant frequency of the mattress and harness system currently used to secure neonates inside incubators is ∼9Hz. This couples to vehicle chassis vibration, increasing vibration exposure to the neonate. The vibration exposure per journey (A(8) using the ISO2631 standard) was at least 20% of the action point value of current EU regulations over all 12 neonatal transports studied, reaching 70% in two cases. Direct injury risk from linear head acceleration (HIC_{15}) was negligible.

Although the overall hazard was similar, vibration isolation differed substantially between sponge and air mattresses, with a manikin. Using a GPS datalogger alongside inertial sensors, vibration increased with vehicle speed only above 60km/h. These preliminary findings suggest there is scope to engineer better systems for transferring sick infants, thus potentially improving their outcomes.

Introduction

Newborn inter-hospital transfer is important in order to provide the centralised neonatal intensive care delivered in many countries. In the UK, over 16,000 neonatal transfers occur every year and these are on the increase. Babies are transferred within a trolley mounted incubator, which is heavily laden with equipment. Secure mechanical fixation of this unit gives gives improved safety in the event of a crash or rapid deceleration, and is provided by mounting points in the ambulance floor into which the trolley is then clamped. However, although these precautions mitigate against injury in the event of a road traffic accident, even in the absence of such events, a number of studies have demonstrated an increased rate of mortality and morbidity following neonatal transfer between hospital sites (1; 2; 3). Of particular concern is the association with brain injury, for example Levene et al found an anomalously high incidence of Intra-ventricular Haemorrhage (IVH) in outborn and transferred, compared with inborn neonates (4). These findings have led to questions regarding other less obvious hazards encountered during transport (5). As the incubators, equipment and staff used during transports are very similar to those in the Neonatal Intensive Care Unit (NICU), and therefore the care provided remains unchanged, it is suspected that vibration and linear acceleration (i.e. mechanical shock) conditions encountered during transport

may be one of the key injury mechanisms. Indeed, a number of animal studies have highlighted the adverse health implications of vibration upon the respiratory system (6) and cardiovascular status (7). In a study of mechanical resonance in the adult brain, Laksai et al stated "our findings suggest a dangerous frequency, around which relative brain motion is maximized" (8). Grosek et al (9) found "an association between daytime road transport and higher heart rate and peripheral blood leukocyte counts, which may be related to some particular (but unidentified) stress of road ambulance transfer" in a study of 48 transports. Hypothetically, this may in turn result in fluctuating blood flow to brain. Fluctuations

[1]Bioengineering Research Group, Faculty of Engineering, University of Nottingham, University Park, Nottingham, UK.

[2]Academic Child Health, School of Medicine, E Floor East Block, Queen's Medical Centre, Nottingham, UK.

[3]Dyson School of Design Engineering, Imperial College London, Exhibition Road, London, UK.

[4]CenTre Neonatal Transport Service, Leicester and Nottingham University Hospitals NHS Trusts, UK.

Corresponding author:

John Crowe, University of Nottingham, Tower Building, University Park, Nottingham, Nottinghamshire, NG7 2RD, UK.

Email: john.crowe@nottingham.ac.uk

in cerebral blood flow are an important mechanism for IVH and subsequent poor neurological outcome (10)

In order to be able to mitigate against the deleterious effects of transport, improved knowledge of the damage mechanism would be beneficial. The relative hazard posed by 'shocks' (that cause rapid relative motion between skull and brain and hence damage to connective tissue), versus relatively long-term continuous vibration (and its effect upon the body's control systems, which may produce physiological responses) are unclear.

A number of previous studies have quantified vibration exposure during inter-hospital transport. Shenai et al (22) studied vibration during neonatal transports using an abdominal accelerometer. RMS vibration power spectral density was computed, concluding that vibration exposure reaches high levels compared to adult workplace limits. Campbell et al (21) measured similar vibration magnitudes, their analysis method differing from Shenai by use of a multi axis accelerometer, whilst Gajendragadkar et al (18) used manikins together with 3 axis accelerometers (on the manikin's head and transport incubator chassis) to measure both vibration exposure during different transport routes, and the isolation properties of mattress configurations. However, these studies did not use standardised methodologies to quantify the hazards associated with whole body vibration: Shenai was limited by single axis measurements; Gajendragadkar failed to validate manikin models against patients; and all three failed to use standardised axis dependent frequency weightings.

This study aims to provide a baseline assessment of the exposure of neonates to head and torso vibrations, and linear accelerations, that is comparable to both current assessments of vibration in the workplace (ISO 2631-1:1997), and to traumatic head injury in vehicle accidents (HIC_{15}). Although extrapolating these adult standards to unwell neonates may be challenging to interpret, it does offer a means of analysis that is well grounded.

A secondary objective is to begin to address the question as to whether transport could be made safer, for example by a redesign of the incubator or its components, or by exerting routing and speed control over the ambulance's journey.

Therefore we will also assess the contribution of the mattress type, the road type, and the vehicle speed upon the vibration exposure to the neonate.

Method

Design and assembly of a datalogger for MEMS inertial sensors

As no off-the-shelf device suitable for use in these studies could be found, a datalogger was custom built to record acceleration and angular rotation rate over the course of neonatal transports and routine vehicle transfers between UK hospital sites. This was a two part device, consisting of 1) a base unit containing the power supply (sufficient for 24 hours operation) and data storage elements, and 2) a set of swappable plug in cable assemblies (2 meters long) incorporating Micro Electro-Mechanical System (MEMS) sensors.

These sensor cables incorporated two small (1cm x 3cm x 2cm) enclosures spaced along their length, with a third smaller sensor board placed at one end, and encapsulated in biocompatible (ISO10993) silicone resin. Each enclosure contained inertial sensors: a three axis accelerometer (ADXL345, Analog devices, Northwood, MA, USA.), and a three axis rate gyroscope with build in temperature sensor (ITG-3200, Invensense Inc., San Jose, CA, USA.). To reduce the size of the resin encapsulated sensor for forehead attachment (where a large sensor could potentially induce resonant modes), a combined accelerometer and rate gyroscope IC was used (LSM330, ST microelectronics, Geneva, Switzerland), this sensor had a 14mm outer diameter and 3 gram encapsulated mass. Fig 1 is a labelled image of the complete system. By incorporating multiple sensor units into a single assembly, aligned datasets could be recorded by a single datalogger, dramatically improving ease of use and reducing the potential for mislabelling in the field.

Fig 2 is a labelled image of the system installed on the 800 gram, 25 week neonatal manikin used in all manikin transports (a LifeForm micro-preemie, Nasco Inc, Fort Atkinson, WI, USA.). The LifeForm micro-preemie is designed to mechanically simulate a neonate, and was employed in the study for ethical reasons where non-standard procedures may have posed a risk. However, mechanical accuracy in terms of vibration transfer is not claimed by the manufacturer.

A "S.K.I.P" harness (SKIP Harness Ltd., 447A Riddell Road, Glendowie, Auckland, New Zealand), which is routinely used as a patient safety restraint is seen in this image.

Manikin and neonatal transports used identical incubator (Draeger Air Shields TI500), and sensor configurations, with one sensor enclosure being attached to the incubator chassis (referred to as the chassis site), one to the torso in contact with the ribcage, and finally the silicone resin encapsulated sensor being secured to the centre of the forehead.

The accelerometers and rate gyroscopes were configured to the largest possible measurement ranges of $\pm16g$ and $\pm2000°s^{-1}$ respectively. These were found to be more than adequate for the conditions encountered during transports, with the magnitude of the largest acceleration being $6.5g$ and largest angular rate being $800°s^{-1}$. It was not possible to run all the sensors at their maximum sampling rates due to hardware limitations, so the head mounted sensor was prioritised, with a high sensor bandwidth of 800Hz used for the LSM330 accelerometer (Table 1). It should be noted that this is still lower than the 1kHz specified in the HIC_{15} standard, meaning that HIC_{15} impacts may have been slightly underestimated by the sensor.

Processing of MEMS sensor data

Analyses of vibration and linear acceleration hazard potential were conducted using the ISO 2631-1:1997 (11) and HIC (Head Impact Criterion) (12; 13) standards respectively. MEMS accelerometers have significant (~0.1g) zero acceleration offsets due to manufacturing tolerances, and their sensitivity typically differs from the published specification by several percent. Offsets typically change with both sensor temperature and device ageing, and so high accuracy calibration can be challenging. For this reason an
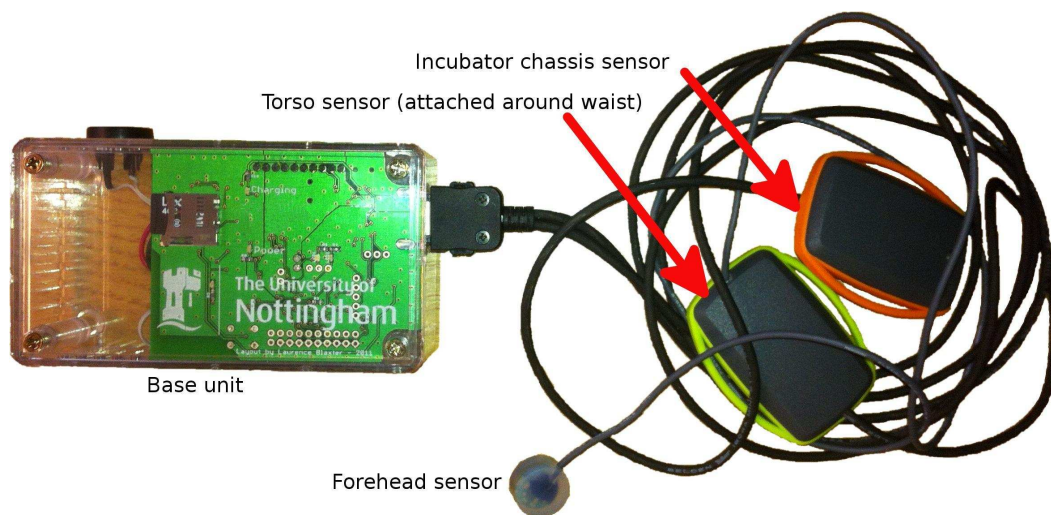
Figure 1. Labelled image of the inertial datalogging system.

Figure 2. Labelled image of the sensors installed on a neonatal manikin.

Location	Sensor type	Manufacturer	Part No.	Sample rate (Hz)	Anti-aliasing filter(Hz)	Raw bits
Forehead	Accelerometer	ST Micro.	LSM330	1600	800	12
	Rate Gyro & Temperature			380	100	16
Torso & Chassis	Accelerometer	Analogue devices	ADXL345	100	50	13
	Rate Gyro & Temperature	Invensense	ITG-3200	100	42	16

Table 1. Summary of sensor configuration.

accelerometer gain and offset compensation algorithm was used to estimate gain and offset correction terms for each accelerometer sensor axis on a per journey basis. The simple 6 point accelerometer calibration process described by Titterton and Weston (14) was trialled for sensor calibration, but required each sensor to be held stationary for several seconds in six different orientations, a complex procedure that was found to be unreliable when attempted in the field.

For this reason a "calibration free" approach was taken, requiring no explicit calibration manoeuvres at any point. The built in $fminsearch$ function from the GNU-Octave environment was used to optimise a six component vector (consisting of 3 offset terms and 3 gain terms) so as to minimize a cost function defined as the median difference between the lengths of the corrected acceleration vectors and 1g. The procedure converges on the correct gain and offset values under the condition that the median true acceleration is of magnitude 1g, and performed reliably in real world application to the recorded datasets.

ISO 2631-1 vibration analysis For the application of ISO 2631 vibration weighting, the horizontal plane frequency weighting function, W_d, and vertical plane function, W_k, were used with torso and forehead data. The motion sickness function, W_f, was not considered as its appropriateness was unclear, and head weighting used W_k as opposed to the W_j head vibration function, as there was a soft pillow beneath the head in all transports. Weightings were applied using scripts running in the GNU-Octave environment, with filter coefficients generated using the procedures outlined by Rimell and Mansfield (15).

As ISO 2631 defines sensor axes relative to a standard body position, movement of the patient and practical considerations when mounting the transducers on the patient created a significant challenge. This problem was overcome using a signal processing algorithm (similar to those used in auto-pilot systems) to track orientation and transform the acceleration data into vertical and horizontal plane components that correspond with ISO 2631 weighting schemes. The three axis sensor data from the accelerometer and rate gyroscope on each sensor were transformed from "sensor body" (x,y,z) or local sensor axis co-ordinates to a fixed "world" co-ordinate system (N,E,D) of fixed horizontal (North, East) and vertical (Down) axes.

The orientation tracking algorithm is illustrated schematically in Fig 3. An Extended Kalman filter (EKF) was used, with a 7 component state vector consisting of three gyroscope bias terms ($\mathbf{b}_{x,y,z}$, the estimated rate gyroscope output in a stationary state), and estimated attitude quaternion (sensor body relative to world co-ordinate system). In most previous strap-down IMU systems, a magnetometer has been used to allow orientation around the vertical axis (yaw) to be determined. No magnetometer was used here, as absolute heading was not required for sensor re-orientation.

The orientation tracker is based on the algorithm described by Foxlin ((16) Fig 2, the "Direct Kalman" approach), with modifications: no magnetometer; and the accelerometer measurement error covariance matrix scaled using the absolute difference between the magnitude of the measured acceleration and a 1g acceleration (i.e. 9.8ms^{-2}). This covariance scaling reduced the influence of prolonged vehicle acceleration on gyroscope bias and orientation; a prolonged period of acceleration leads to a non vertical acceleration vector (biassing the filter), but also to an acceleration with magnitude greater than 1g, allowing such acceleration events to be identified and assigned a high error when input into the EKF.

Once the acceleration vectors had been rotated into the NED frame (A_{world} in the figure), it was assumed that the patient was in a reclining position, and that the ambulance chassis was horizontal. Although neither of these conditions will be completely satisfied in practice, it was judged that any deviations of the vehicle from horizontal were likely to be of short duration and limited tilt angle (likely <5°), making them a less significant cause of mis-modelling than imperfect patient orientation relative to a true reclined position, an error source that cannot easily be controlled. It should also be noted that the ISO 2631 specification states that "the sensitive axes of transducers may deviate from the preferred axes by up to 15° where necessary". In the world or NED frame, North was treated as patient z axis, East as patient y, and Down as the patient x axis. The ISO 2631 weighting filters could then be applied (using the algorithm described by Rimell and Mansfield (15)), giving weighted outputs at the raw accelerometer sample rates.

Further windowing of weighted data into 10 second intervals, followed by calculation of the RMS vibration on a per window basis was then undertaken, allowing analysis of vibration as a function of road class and vehicle speed, with the ten second period being chosen based upon consideration of typical vehicle acceleration. Calculation of crest factor and eight hour equivalent vibration exposure, or A(8) proceeded as per ISO 2631 (7.2.3).

HIC$_{15}$ analysis of linear head acceleration The Head Impact Criterion (HIC) is defined by the NHTSA (National Highway Traffic Safety Administration) (13), Chapter 2. HIC is the acceleration in g units integrated with respect to time over a rolling window, and raised to the power of 2.5 following normalisation with respect to the integration period (equation 1). HIC can be defined over arbitrary window lengths, these usually being denoted in ms using a subscript. HIC$_{15}$ was implemented as 15ms is a common window length, used in for example the EEVC working group report (17).

$$HIC = (t_2 - t_1) \left[\frac{\int_{t_1}^{t_2} a(t)dt}{t_2 - t_1} \right]^{2.5} \tag{1}$$

HIC$_{15}$ was assessed using the head sensor accelerometer. A rolling window method was used to process the A_{world} accelerometer data (which was gain and offset compensated and rotated into world space, but not changed in magnitude by the quaternion rotation), with local maxima of HIC above a threshold of 0.3 being logged.

Although extrapolation of HIC$_{15}$ thresholds down to neonatal patients is difficult, extrapolation to newborn and 12 month old subjects has been attempted, for example Eppinger et al suggested a limit value of 390 for 12 month old subjects (13), and noted that values as low as 200 have been suggested elsewhere. Using the formula $\lambda_{HIC} = \lambda_{\sigma f}^{2.5} - \lambda_L^{-1.5}$, where λ_{HIC} is the scaling factor for HIC, $\lambda_{\sigma f}$ is for tissue mechanical maturity, and λ_L is for length, Johannsen et al (19) discuss scaling of HIC with age (from the validated Q3 dummy, and with data from the CASPER project). Using tensile strength data for a 22 week foetus and the dimensions of the manikin used in this study gives a scaling factor of $\lambda_{HIC} = 0.13$. Applying this scaling factor to those validated for the Q3 dummy gives injury thresholds of HIC$_{15}$=99 and 130 for 20% and 50% risks of an AIS 3+ injury respectively. The European Enhanced Vehicle-Safety
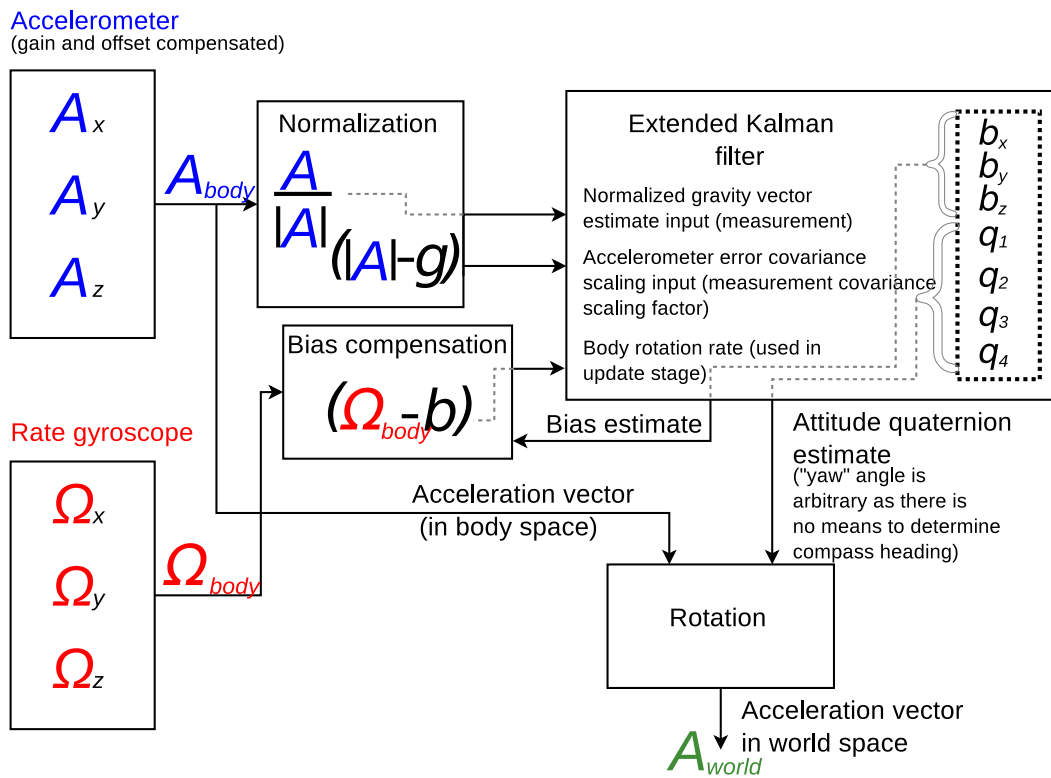
Figure 3. Flow diagram showing data flow through the orientation tracker.

Committee (EEVC) working group 12 and 18 report ([17](#)) reaches very similar figures using the CHILD project dataset.

Analysis of vehicle speed and road class An off-the-shelf GPS datalogger (M-1200E, Holux Technology Ltd, Taiwan), installed in the vehicle cab recorded vehicle position and velocity over the course of all journeys. As data collection took place over several months, a correlation technique (between vibration and GPS vehicle speed) was employed to ensure correct data alignment (to within 5 seconds).

Road classification used the open access "nominatim" server run by openstreetmap (nominatim.openstreetmap.org/reverse) to convert GPS positions to location descriptors, which were then passed back to the server to find the nearest object described as a "way object" (implying a road). As this takes several seconds, optimised querying was employed: the raw GPS data (a 1Hz time series record) was interpolated to a physically uniform sequence of points, one per 100m of travel, and binary search applied to identify transition points between road classes with minimal queries. Retrieved "way objects", passed back from the server as xml files, were finally processed with string matching, and classified as one of nine road types; motorway, expressway, trunk, primary, secondary, tertiary, tertiary link, service and unclassified.

To explore the influence of road class and vehicle speed upon vibration, the 10 second RMS weighted vibration intervals were matched to the corresponding road class and vehicle speed, and then binned to calculate the total number of intervals (and thus travel duration) falling within a range of RMS vibrations ($0.1\mathrm{ms}^{-2}$ increments), and vehicle speeds (10km/h increments) for the entire dataset.

Selection of patient and manikin transports

A convenience sample was recruited, consisting of infants requiring transfer by the CenTre transport service between Trent Perinatal Network neonatal units. Patient inclusion criteria were pragmatic, including all infants who were cared for in a neonatal unit and required transfer, but excluding those undergoing palliative care. Manikin studies took place on ambulance journeys when no patient being transferred (i.e. before or after transferring a patient), allowing these journeys to serve as direct validators: using the same transport system, vehicle, and routes. The CenTre service routinely uses a sponge mattress for transfer and a "S.K.I.P." harness as the patient safety restraint.

To investigate the influence of mattress type upon vibration, the manikin studies were divided into three groups, which used: the stock Draeger incubator mattresses, a polyurethane foam material (sponge) also used in all neonatal patient transports; gel mattresses (Squishon, Philips Healthcare); and air mattresses (Repose Babynest, Frontier Therapeutics, Blackwood, UK).

The journeys studied were within a group of 16 hospital sites, and all but four of the routes were unique. The UK transport fleet consists of numerous vehicle types, but to minimised confounding effects, transports were constrained to a single vehicle make and model: Volkswagen LT-35 (3L diesel). The LT-35 has dual wishbone front suspension with a leaf sprung rear live axle, a layout used in most of the UK vehicle fleet, and identical to the Chevrolet P-30 employed in a previous study by Shenai et al ([22](#)).

Informed consent was obtained in writing from the patient's parents or legal guardian before all neonatal patient transports commenced.

Results

Data was recorded from a total of 35 ambulance journeys, 12 of which were neonatal transports, with the others using the manikin. Total duration was 34 hours, with journey distances being between 45km and 200km. The 12 neonatal transports involved a total of 10 patients, birth gestation range 24+2 to 41+2 weeks, and weight range 0.9-4.6 kg, median 1.9 kg.

The forehead sensor data from three manikin journeys was found to be corrupted due to intermittent faults with the sensor cabling, leaving 32 journeys with data from all three sensor sites. Out of the manikin transports, 10 (including 8 with forehead sensor data) used a sponge mattress, 7 (6 with forehead sensor data) a gel mattress, and 6 an air mattress.

Frequency space vibration analysis

Fig 4 shows a spectrogram (using ten second bins) of vibration at the forehead site over the course of a typical manikin transport with sponge mattress. The x, y, and z sensor axes are mapped to red, green, and blue respectively in the image, meaning that the colour separation indicates vibration along different axes.

Several features correspond to events noted during the ambulance journey: 1) periods of very low vibration when the vehicle was stationary (vertical bands, e.g. at time A), with the engine idling during some of these (e.g. time B), this leading to horizontal line C at approximately 7Hz with 14Hz harmonic D; and 2) short periods of broad spectrum noise. There are two short periods of broad noise, at times E and F, which correspond to times when the manikin and datalogging equipment was repositioned, leading to short mechanical shocks. The vibration occurs along two distinct bands; G at 1.5Hz, and a band spanning 6.5Hz (H) to 13Hz (I). This second band has clear colour separation between H and I, indicating that the vibration axis is frequency dependent and thus this band may be the result of multiple resonances. Most vibration energy was concentrated between 5Hz and 20Hz. The fact that colour of the engine vibration harmonics during of idling matches that of the bands at approximately 7Hz and 14Hz (when the vehicle is in motion) suggests that these bands may originate from the engine, as the vibration direction is similar. The lower frequency band G appears to arise from resonance of the vehicle suspension.

In Figs 5 and 6, vibration spectral density has been plotted following subdivision of the data according to sensor site, axis (horizontal plane or x/y, and vertical or y axis), and journey type. Journeys were divided into four types; three manikin types according to mattress configuration (sponge, gel, or air), and neonatal transports as a fourth group (these used the sponge mattress). For each sensor site and each axis, RMS vibration spectral density was calculated by averaging the appropriate data from all of the journeys of each of the four journey types. These types are indicated according to the figure key. Two very distinct vibration peaks can be seen in the figures. The lower frequency peak aligns closely with the band identified earlier in the spectrogram as G, and likely originating from resonance of the vehicle suspension. The higher frequency peak spans the 7 to 14Hz region which was earlier identified as likely originating from the engine and transmission. The small spike at 26Hz in the neonatal transports was found to have originated from

an incubator ventilation fan which was turned off during manikin transports. The vertical axis spectrum at the torso site recorded during neonatal transport (Fig5b) shows very good agreement to the results published by Shenail et al ((22) Fig 1) who used a piezoelectric accelerometer with a 2Hz to 30Hz bandwidth at the same sensor site.

Compared to the incubator chassis, spectral density in the 3 to 20Hz range is up to four times higher at the torso and forehead sensor sites, indicating that vibration is amplified over this spectral range. This finding is in agreement with a previous study by Gajendragadkar et al (18), in which the mattress system amplified vibration magnitude by factors of between 2.2 to 3.4 (sponge) and 1.1 to 2.1 (gel type). However, this previous study is not directly comparable, as it compared RMS values computed from 50Hz low pass filtered acceleration data.

To analyse exposure hazard, a model was used consisting of an input "chassis level" function (the RMS vibration spectral density at the chassis site), passed through a frequency dependant weighting function (W_k or W_d as per ISO 2631), and finally through a site and configuration dependent gain function (computed from the study data) modelling resonant effects between the incubator chassis and the neonate or manikin. Overall RMS vibration at the head and torso sites could then be calculated for the various mattress configurations. Compared to a direct comparison of weighted RMS vibration between study groups, this method reduces confounding effects from journey to journey variance in chassis vibration, allows for insight into the origin of the vibration hazard, and enables evaluation of configurations that were not part of the original dataset. It may thus be possible to extend the analysis to configurations such as neonate with air mattress, although this was not attempted as differences between the manikin and neonates were minimal.

Fig 5c shows a 45% reduction in the amplitude of the 1.5Hz peak during neonatal transport. It would appear that drivers may have been more attentive to road conditions and vehicle vibration during patient transport, a hypothesis supported by the reduction in both frequency and amplitude of the higher frequency (engine vibration related) peak. For this reason two "chassis level" spectral density functions were generated, one from manikin transports, the other from neonatal transports.

Application of the frequency weighting functions W_k and W_d to the chassis vibration is illustrated in Fig 7 as the "Weighted level". The peak in vertical axis weighted vibration spectral density at around 12Hz can be seen to dominate this damage potential function. Mattress configurations, driving styles, or vibration damping arrangements which minimize the amplitude of this peak, would appear to be a promising route forward if a reduction in overall vibration exposure level is desired.

The vibration gain functions were calculated between the incubator chassis, and the forehead and torso sensors by dividing torso and head spectral density functions by the chassis spectral density. This allowed for assessment both of the effects of different mattress configurations upon vibration attenuation, and of the validity of the manikin as a mechanical model through comparison with the neonatal patients.
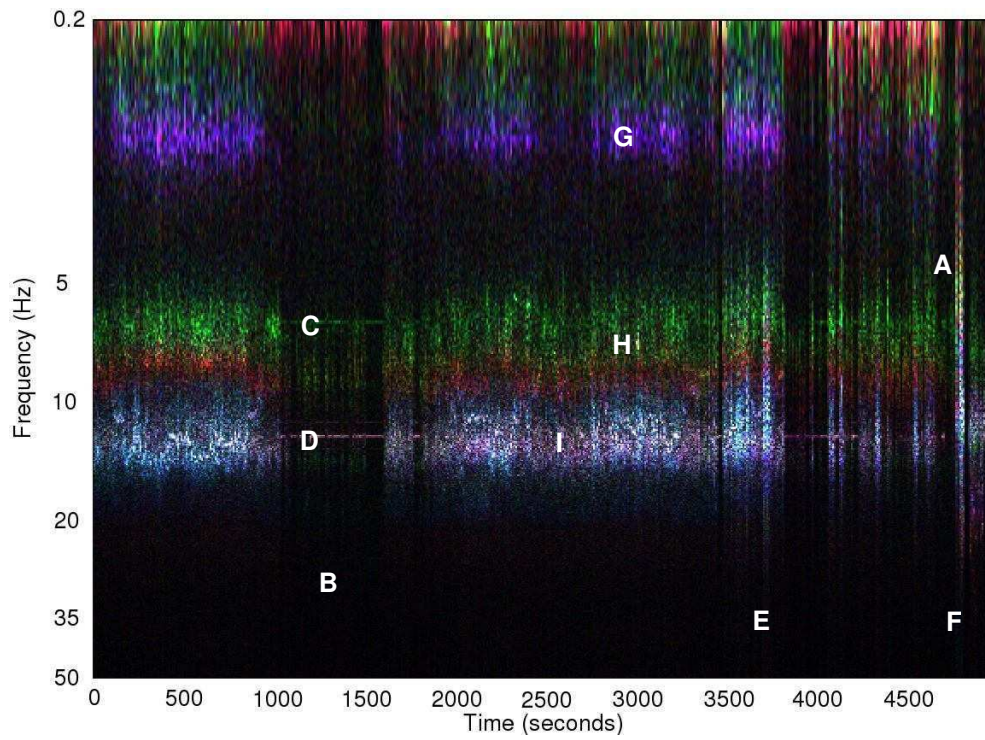
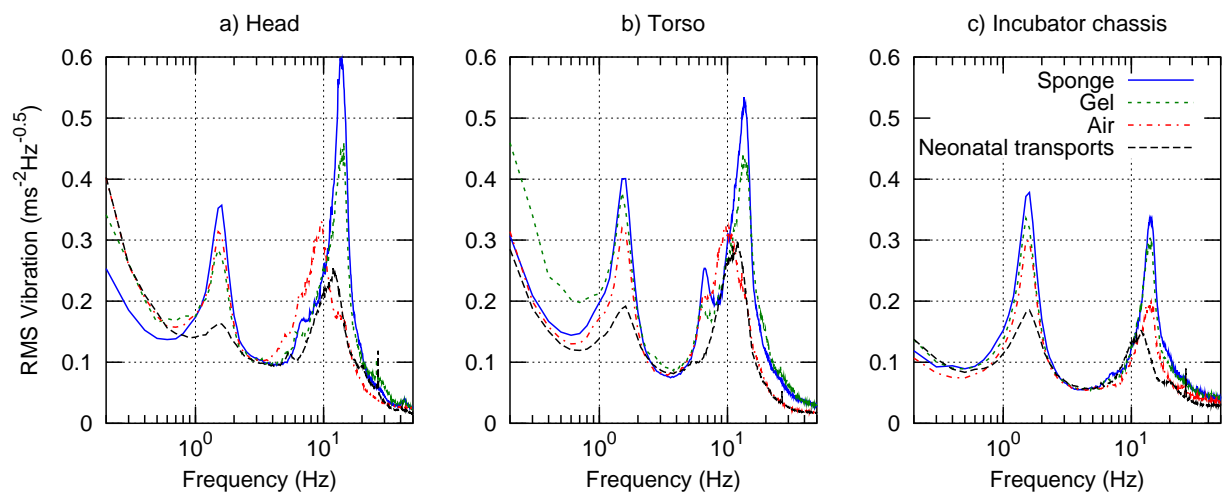**Figure 4.** Spectrogram of raw acceleration during a typical transport, forehead site.

Figure 5. Spectrum of vertical (z) acceleration magnitude, all three sites and four journey types.
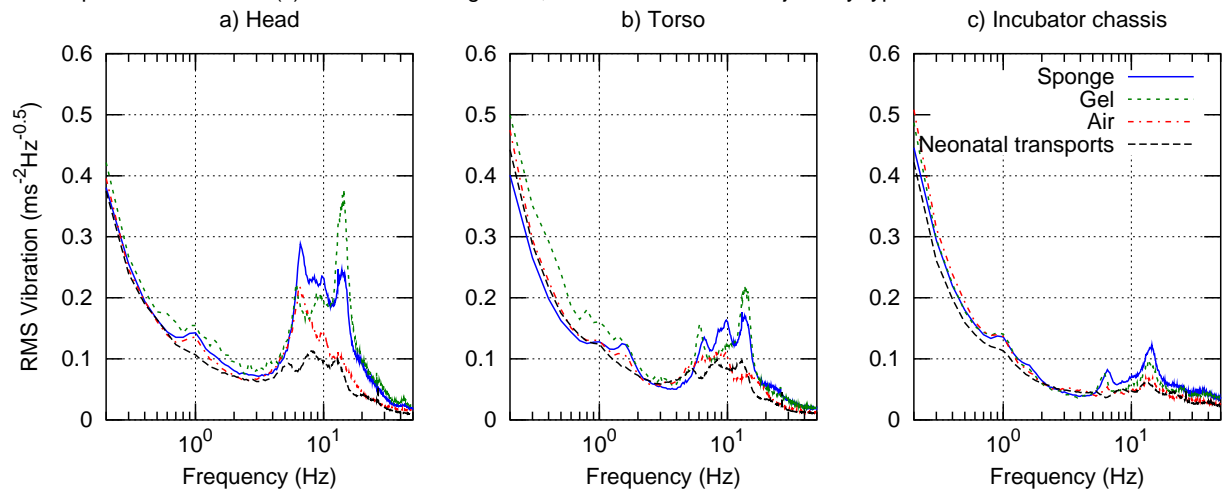

Figure 6. Spectrum of horizontal plane (x, y) acceleration magnitude, all three sites and four journey types.
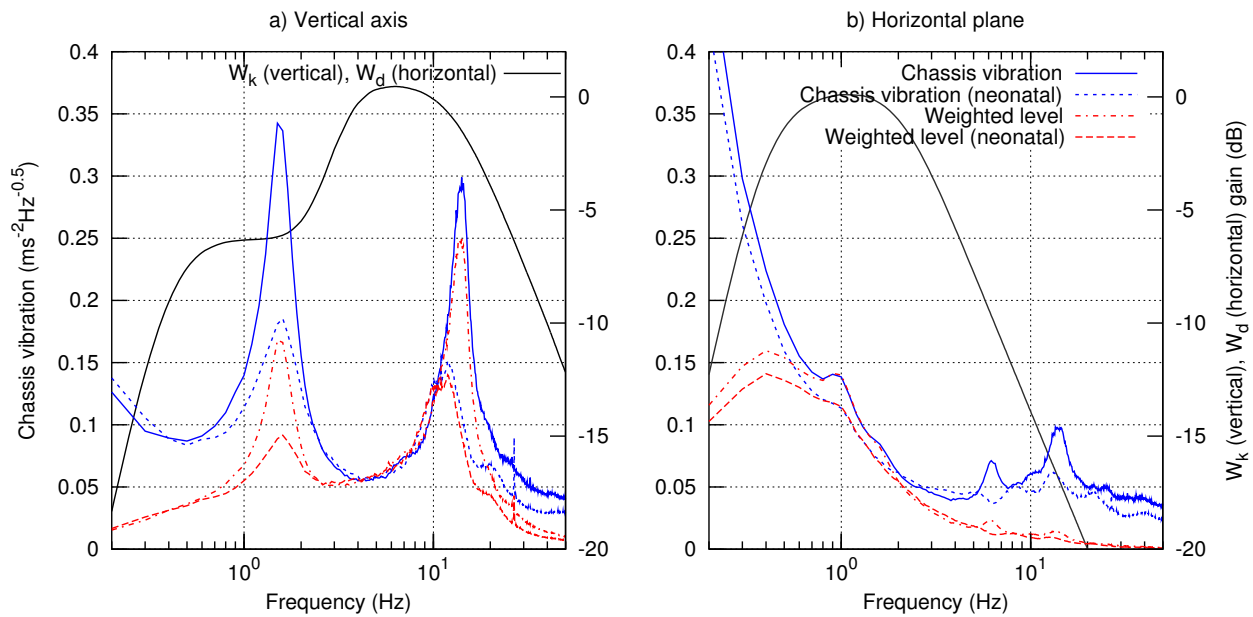
Figure 7. RMS chassis vibration in vertical axis and horizontal plane, before and after application of ISO 2631 weighting functions W_k and W_d.
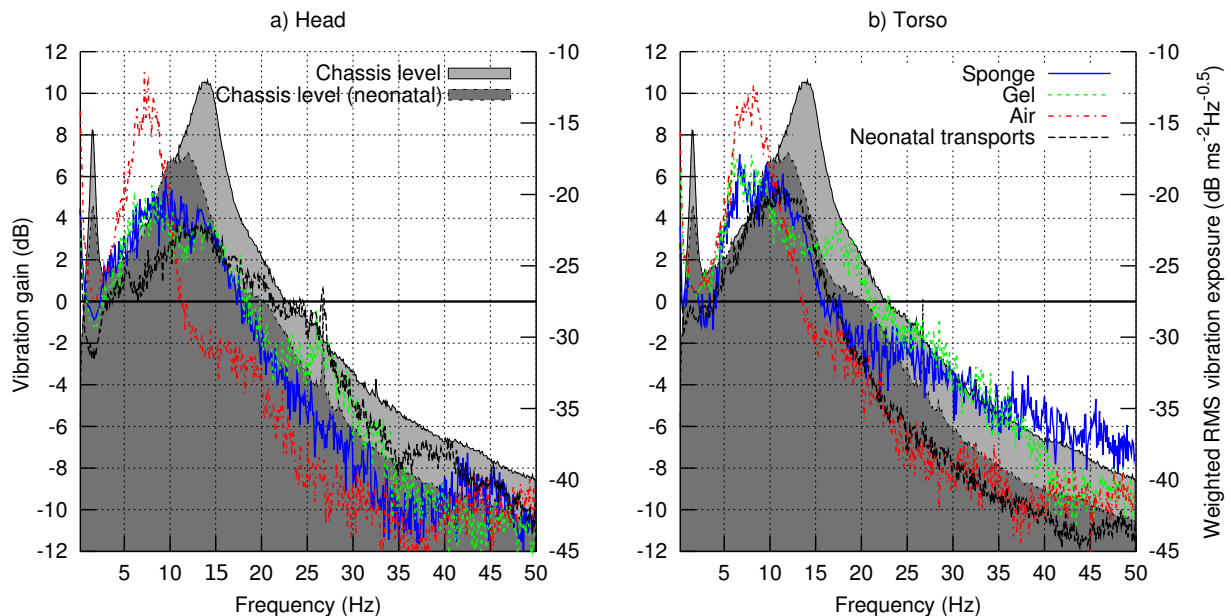

Figure 8. Vertical (z) acceleration gain between incubator chassis and neonatal and manikin head sensor.

Fig 8 plots vibration gain between the incubator chassis, and both the manikin (with sponge mattress) and the neonatal patients. Although the two gain functions deviate by up to 3dB (~40%) in places, there is a less than 1dB (~10%) deviation over the 10Hz to 18Hz frequency band, where gain is highest and the majority of the damaging vibration is concentrated (Fig 5c). The spike around 26Hz in the neonatal trace is caused by the raw data peak identified earlier (and originates from a fan). Given the close match between gains, it appears that the manikin is an appropriate model for the assessment of neonatal vibration exposure. The close match is also notable given the large range of patient masses across the study group (0.9-4.6 kg), which did not overlap with the 0.8 kg manikin mass. This indicates that patient mass only weakly affects vibration damping, and that the heterogeneity

of the sample group is unlikely to have a significant impact on the results..

Vibration gain (in decibels) was also calculated between the incubator chassis and the forehead and torso sensor for the four different journey types, and is plotted in Figs 9 and 10. The plot lines (left hand side axes), are vibration gains in dB, and the dB scaled chassis sensor vibration spectral density, or "Chassis level", is plotted as a shaded background (right hand axes). A gain peak (indicating resonance) is seen at 7Hz for the air mattress and around 10Hz for the other mattress configurations, with a peak gain of between 3 and 5dB in the vertical axis for both the sponge and gel mattress, and the neonatal transports, with a considerably higher peak for the air mattress in the vertical axis (10dB for the head at 7Hz). The response rolls off at higher frequencies at approximately 15dB per decade in the vertical axis (i.e.
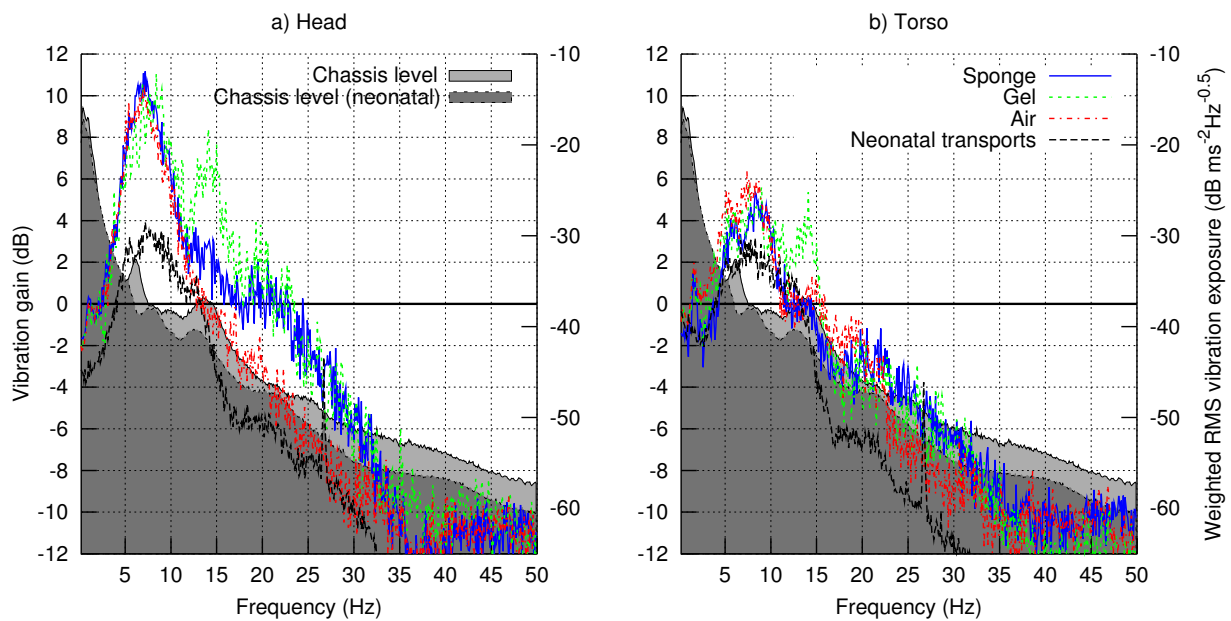
Figure 9. Vertical (z) acceleration gain between incubator chassis and head (a), torso (b). Plotted versus frequency for all four journey types.
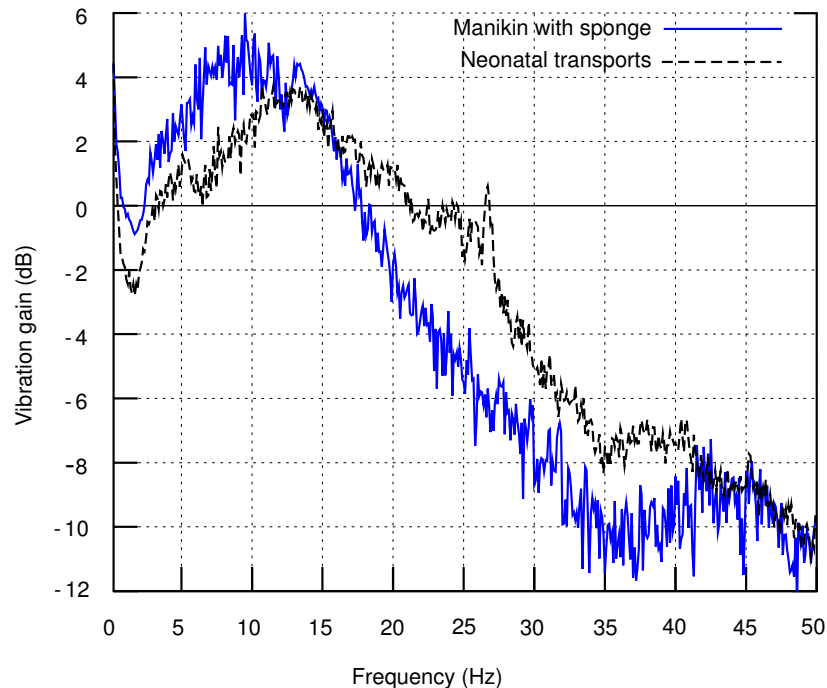

Figure 10. Horizontal plane (x, y) acceleration gain between incubator chassis and head (a), torso (b). Plotted versus frequency for all four journey types.

slightly lower than a first order roll off), and around 20dB per decade in the horizontal from 5 to 35Hz (first order).

It is notable that, although there is a 7dB peak at 14Hz in the horizontal axis for the gel mattress which is not present for the sponge mattress, the vibration gain of the gel mattress is similar to the sponge mattress, with the gel gain being within 2dB of the sponge over most of the plotted frequency range, thus suggesting that the sponge and gel mattresses are mechanically similar. It is suspected that the large 7dB deviation in horizontal plane attenuation at the head site around 7Hz (where the large resonance peak is strongly damped in the neonates) may be related to the different procedures used to secure the neonates as compared to the manikins; for the neonatal transports, air lines etc. need to be attached, changing the mechanical coupling to the head.

Another significant feature seen in the two vertical axis gain plots is that peak gain occurs at a lower frequency than peak "Chassis level" (i.e. chassis vibration spectral density during manikin transports) for all four transport types. For neonatal transports the peak vertical vibration density, or "Chassis level (neonatal)", occurs at approximately 12Hz, lower than the 14Hz peak of the "Chassis level", and roughly coinciding with the resonance peak of both the sponge and gel mattress with manikin, and the neonate (with sponge mattress) configurations, meaning incubator chassis vibration will drive the mattress and manikin/neonate system

on resonance. However, as the peak in air mattress gain is at a considerably lower frequency of 7Hz, it avoids such an effect.

Finally, the two frequency weighted chassis vibration spectral density functions (Fig 7) were scaled using the vibration gain functions (Figs 9 and 10), and the overall RMS vibration at the head and torso sites calculated for the four mattress configurations (manikin with sponge, gel, and air, neonate with sponge) and two chassis level functions (for manikin and neonate driving styles).

The resultant RMS vibration is plotted in Fig 11. Several features are seen: the vertical axis vibration dominates overall exposure; the small changes in driving style during the neonatal transports reduced vibration magnitude by approximately 30%; the air mattress results in an increase in vibration exposure with the neonatal driving style; and there is virtually no difference between the manikin with sponge mattress, manikin with gel mattress and neonate with sponge mattress. Use of an air mattress results in only a modest ($\sim$ 15%) reduction in vibration with the manikin driving style. RMS vertical axis vibration is well above the 0.315ms^{-2} comfort limit specified in ISO 2631, with horizontal plane vibration falling well below this limit.

Thus, as well as illustrating the severity of the vibration experienced during neonatal transport, these preliminary results also suggest that replacement of sponge mattresses with air or gel mattresses may not be beneficial; the gel mattress does not result in any significant reduction in vibration exposure, and the air mattress results in slightly increased vibration exposure when the vehicle is driven within a low engine rpm range. Furthermore, the gel mattress has a considerably higher density (approx 1gram/ml) than the sponge (approximately 0.2grams/ml), presenting an increased risk of injury in the event of a road traffic accident.

HIC_{15} data

HIC_{15} values were extremely low across the entire dataset. For this reason a more detailed analysis of the HIC_{15} data was not conducted. Out of the 12 transports with neonatal patients, HIC_{15} exceeded a threshold of one on only four journeys, with a maximum value of 9.3 being seen at the forehead sensor on one journey. The majority of patient transports saw no HIC_{15} impacts above a threshold of 0.3, and the maximum HIC_{15} at the forehead sensor site during manikin transports was 13.1. These values are well below both the accepted limit value of 700 for adults (13), and the scaled value derived in section of 99 for 20% risk of AIS 3+.

Since the maximum HIC_{15} values for neonatal (9.3) and manikin (13.1) transports were an order of magnitude smaller than these thresholds, it would appear to be highly unlikely that linear acceleration shocks will directly lead to significant traumatic head injury.

A(8) exposure statistics

The A(8) metric is defined in ISO 2631, and measures cumulative Whole Body Vibration (WBV) exposure, normalized to an 8 hour equivalent period using a nonlinear scaling. WBV is defined as the quadratic mean of the weighted horizontal plane and vertical axis vibration. The EU vibration directive defines a daily exposure action value

of 0.5ms^{-2} for A(8) occupational exposures to whole-body vibration (Griffin et al (20)).

ISO 2631 warns that A(8) may prove inaccurate in the case of a high crest factor (the ratio of peak filtered vibration magnitude to RMS vibration over the exposure interval). A fourth power integration method is suggested as more appropriate in cases where crest factor is greater than 9, but fourth power exposure values are more difficult to interpret. Crest factor was calculated on a per journey basis, and was greater than 9 for the majority of transports (Fig 12).

As it was hypothesised that crest factors may be biassed by a small number of acceleration events during vehicle loading and unloading, the raw acceleration data was processed to locate instances of high acceleration. This analysis is plotted in Fig 13, and supports the hypothesis, with shock events clustering around the start and end of journeys. Note that sensors were secured to the manikin or neonate prior to the datalogger being turned on, and before the transport trolley was then loaded into the transport vehicle. This process was repeated in reverse order once the vehicle reached its destination, with the datalogger turned off prior to sensor removal. Thus the captured events are believed to represent real accelerations, rather than simply attachment and removal of the sensors. Exclusion of 5% of the data at the beginning and end of each journey to avoid inclusion of these clusters lowered median head crest factor to 7.8 and torso to 8.9. For these reasons it would appear that A(8) is an appropriate means of assessing cumulative exposure, as median crest factors over the middle 90% of the transport period (when the vehicle was in motion and the patients were exposed to the majority of the hazardous vibration) are below 9.

A(8) exposures were calculated from the weighted acceleration data on a per journey basis. From Fig 14a and 14b, 2 journeys saw an A(8) vibration exposure magnitude greater than 0.5ms^{-2} at the forehead. These did not include any neonatal transports. Vibration exposure to the torso was slightly worse, with 4 transports exceeding 0.5ms^{-2}, although again this included no neonatal transports. Nevertheless, the fact that neonatal exposures approach the workplace exposure limit for healthy adults would appear to be a significant cause for concern.

Analysis of vibration versus vehicle speed and road class

Vehicle vibration is plotted versus vehicle speed and road class in Fig 15. The binning procedure used in this analysis was outlined in section . As a relatively large period of time was spent with the vehicle at low speeds on minor roads, a logarithmic colour bar has been used in one of the figures for clarity.

Maximum recorded vehicle speed was 131km/h, with 99% of travel time spent below 112km/h (70mph), and a median speed of 75km/h (47mph). Vehicle speed was strongly related to road class; speeds exceeded 90km/h over only a very small proportion of A road travel time, whereas almost all motorway and expressway class travel was between 80 and 120km/h, and most minor class road travel was below 50km/h. This complicates any analysis of the effect of road class upon vibration. At a given speed, vibration might be expected to be inversely related to road grade, but any such
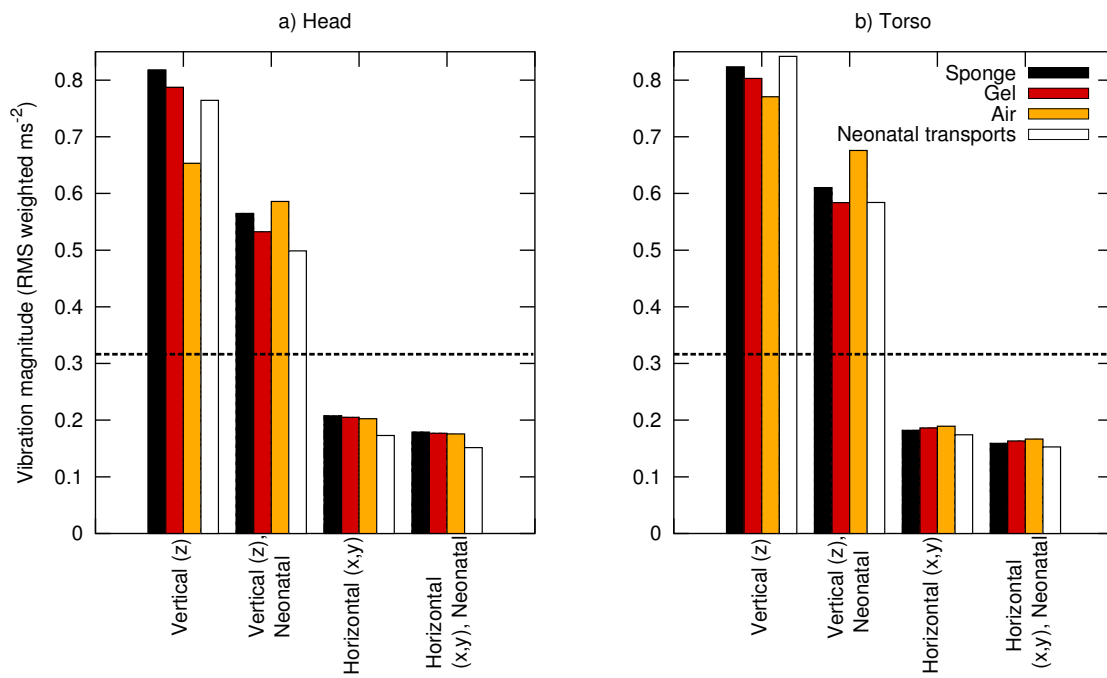
Figure 11. RMS vibration in vertical axis and horizontal plane, after application of ISO 2631 weighting functions and vibration gain to the two chassis vibration density functions. The dashed horizontal black line de-marks the ISO 2631 "comfort limit" of 0.315 ms^{-2}.
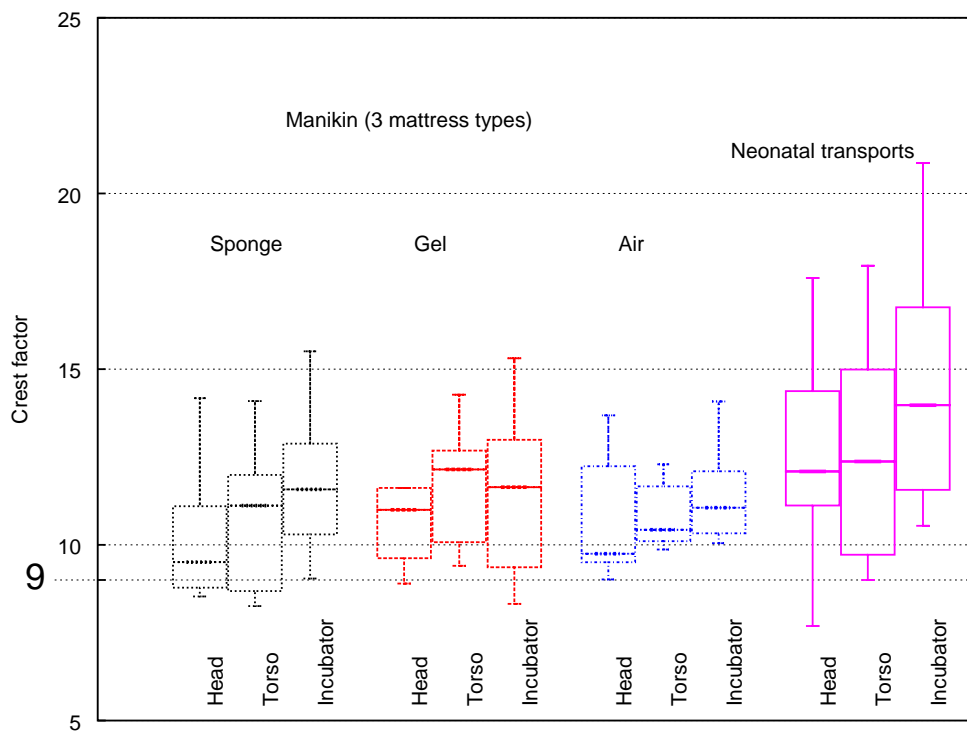

Figure 12. Crest factors (ISO 2631 standard).

effects appear to be small. Comparing Figs 15c and 15a, lower class roads have a slightly higher median vibration at vehicle speeds between 5 and 50km/h, suggesting a poorer ride on B and lower class roads. Any comparison in ride quality between A and expressway/motorway classes (Fig 15b) is impossible as there is no significant overlap in speed ranges. From Fig 15a, the vibration distribution during periods when the speed was 0 to 10km/h is very similar to that at speeds below 70km/h. As the engine was usually idling when the vehicle was stationary (e.g. Fig 4), this suggests that engine vibration may be the most significant vibration source at these speeds.

Although it complicates analysis of the influence of road type upon vibration, the very strong dependence of speed upon road type leads to important conclusions regarding choice of transport route; for example if a speed above 85km/h is desirable, then a route involving express-way or motorway class roads should be chosen, as lower speeds are
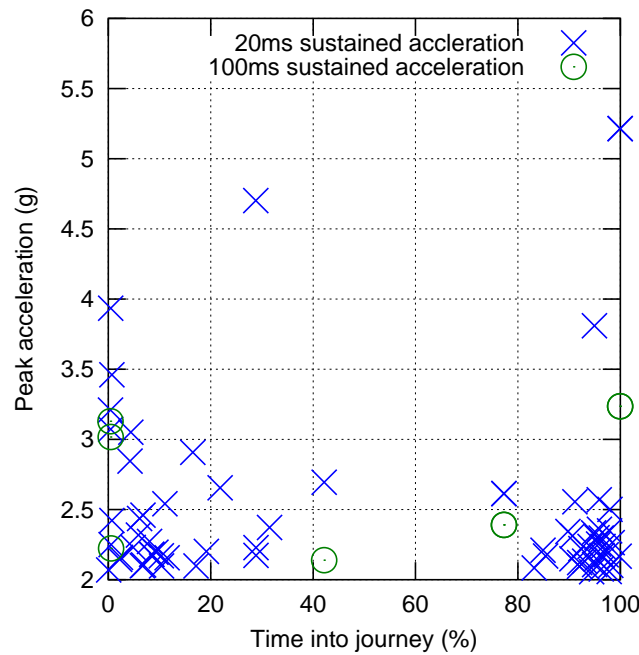
Figure 13. Shock events (defined as a greater than 2g acceleration sustained for more than 20 or 100ms) over the course of all transports, time normalised to journey duration.
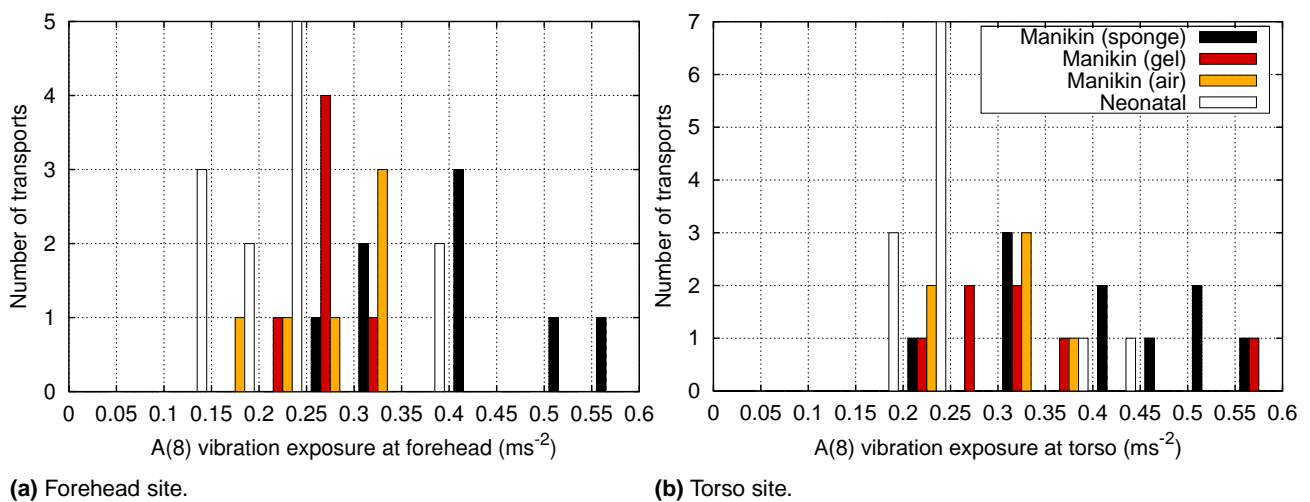

(a) Forehead site.

(b) Torso site.

Figure 14. Histogram of A(8) exposure for all journeys.

found on 'A' classes. To further investigate the relationship between vehicle speed and exposure, the median and quartiles of the weighted forehead vibration were calculated as a function of vehicle speed (using all data recorded over all road classes), and are plotted in Fig 16 (left subplot).

As speed increases, a continual upward trend in vibration is evident, with an increasing gradient. To model the potential influence of vehicle speed upon health risk, the vehicle range (in km) before the cumulative A(8) exposure to the patient exceeded a threshold of 0.5ms^{-2} was calculated for each vehicle speed. Range at the median exposure level is plotted as the blue dashed trace (on right subplot), and the quartile as the green dashed trace.

From the figure it can be seen that a vehicle speed below 60km/h would increase A(8) exposure, due to the increased journey time. Optimal vehicle speed is unclear; the median range peaks at a speed of 110km/h, so it appears that vehicle speed above this results in higher A(8) for a given journey

distance, but there is a considerable amount of oscillation in the median line. However, vehicle speed in the 80 to 110km/h range appears to be near optimal.

In summary; simply restricting maximum vehicle speed to the UK motorway limit of 113km/h, and otherwise driving at the highest speed road conditions allow is likely to result in minimization of vibration exposure to patients during transport. Transport distances should be limited to below 200km (125miles) or shorter if there is likely to be significant travel at <60km/h (37mph). Routes should be chosen to minimize duration rather than distance.
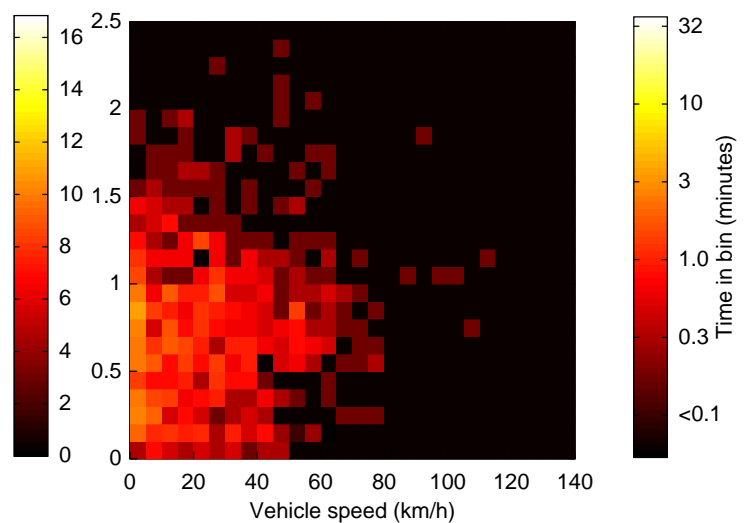
Conclusions

We have demonstrated that a custom made datalogging system for use with MEMS sensors can be successfully deployed in the field to measure shock and vibration during routine neonatal patient transports between UK hospital sites. Data has been recorded at an appropriate sample rate
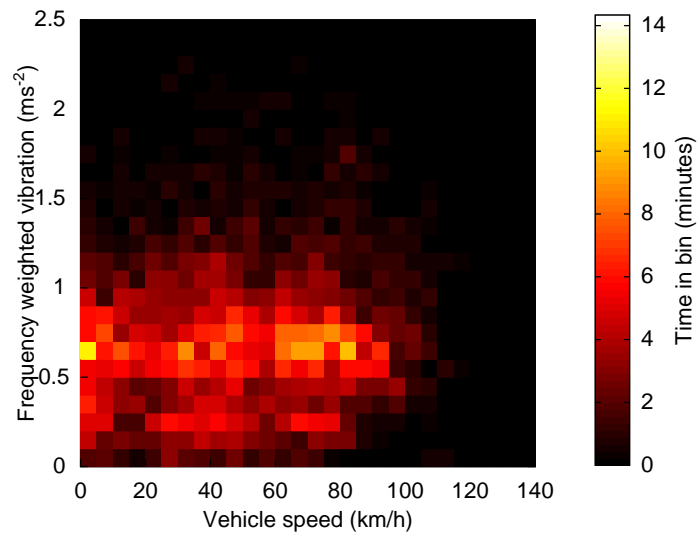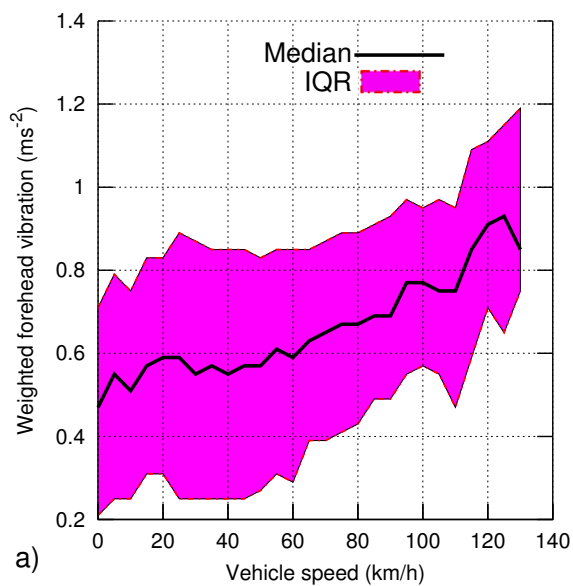
(a) 'A' and trunk road classes
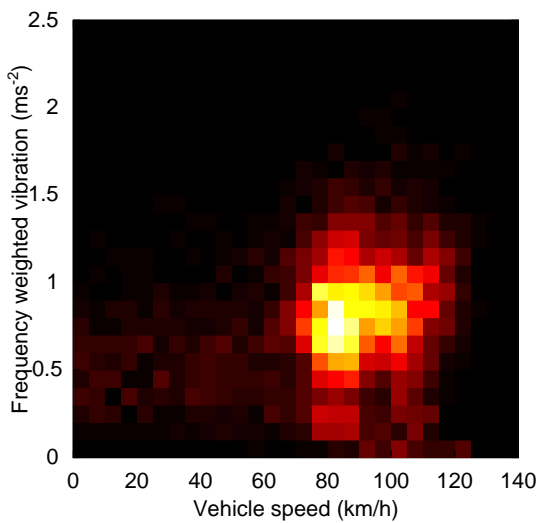
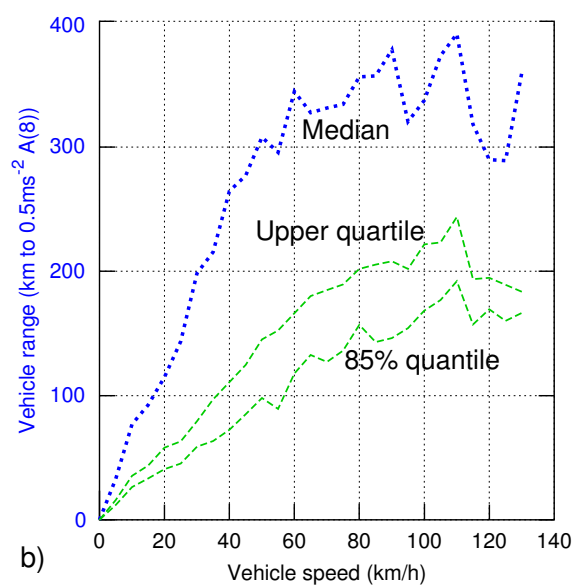**(b)** motorway and expressway classes

(c) remaining (lower) road classes (logscale).

Figure 15. Forehead vibration versus speed.

a)

b)

Figure 16. Median vibration and quartiles versus vehicle speed (a), and vehicle range before A(8) exposure limit exceeded (b).

for the duration of a total of 35 journeys, of which 12 were neonatal transports, and the remainder inter-site vehicle

transfers using a manikin together with three different mattress configurations.

Throughout this study, vibration assessment standards designed for adults in the workplace environment have been employed. This was done out of necessity, since commonly agreed methods for assessment of vibration in neonatal patients do not exist. Unfortunately it is not possible to accurately extrapolate to significantly lower body masses, and so the precise levels of hazard identified here are unclear, as are the likely mechanisms of damage. Standardised assessments for neonatal vibration hazard would aid risk quantification enormously.

Data analysis using HIC_{15} to quantify linear head acceleration hazard, and ISO2631-1:1997 for vibration hazard, indicates that shock exposure is negligible but that vibration exposure approaches and sometimes exceeds the $0.5ms^{-2}$ A(8) "action value" threshold for adults in the workplace, as defined in EU regulations. These findings broadly agree with previous studies of vibration during neonatal transport, for example Campbell et al found RMS accelerations between $0.4ms^{-2}$ and $5.6ms^{-2}$ [21], with the vehicle transports (air transport was also studied) being towards the lower end of this range. Shenai et al found values between $2ms^{-2}$ and $6ms^{-2}$ [22], higher than in our work. The age (1974 model year) of the vehicle used by Shenai suggests improvements in vehicle construction may explain this.

We have not explored influences of vehicle suspension upon vibration conditions, however the spectral analysis indicates that engine as opposed to wheel vibration is the dominant hazard source, implying that engine mounts are a determining factor as opposed to vehicle suspension.

Comparison of the incubator chassis to forehead gain functions between manikin and neonatal study groups shows good agreement, with <2dB deviation in the 10Hz to 20Hz band where the majority of vibration hazard is concentrated. This implies that the manikin is an acceptable mechanical model. Manikin data indicates that vibration exposure during incubator transport is not reduced significantly by replacement of the current sponge mattresses with air or gel mattresses. Replacement with air mattresses results in increased vibration exposure under some driving conditions, and the high density of a gel mattress may increase injury risk in a road traffic accident.

Using a GPS datalogger in the vehicle cab, the influence of vehicle speed and road type upon vibration exposure has been investigated. Optimal speed range for minimization of vibration exposure appears to be between 80 and 110km/h (50 to 68mph), with vehicle speed below 60km/h (37mph) increasing overall exposure due to the longer journey time.

Road type appears to weakly influence vibration, as lower class roads (UK 'B' and below) give higher WBV for a given vehicle speed. A reduction in total vibration exposure might be achieved through optimisation of transport routes, for example longer routes involving 'A' and motorway class roads could be adopted in place of shorter routes involving minor roads, although this concept would require further analysis to assess its feasibility.

As the most hazardous vibration is in the 5 to 20Hz frequency band, which can be damped with simple mechanical shock absorbers, improved transport trolley and incubator design may be the most promising route for reducing patient vibration exposure. The vertical axis resonant frequency of the incubator/mattress system was approximately 10Hz with a sponge or gel mattresses, with around 5dB peak gain between incubator chassis and the torso and forehead sites. This frequency lies close to the 14Hz chassis vibration peak, believed to originate from the engine and transmission, and so is easily excited. Mattress induced resonance was highlighted in a previous study by Gajendragadkar et al [18], who found vibration gain factors which are comparable to those measured in this study. However, this is the first study to demonstrate, in real patients, that the neonatal head is exposed to mechanical vibration hazard in excess of that simply observed at the incubator chassis.

Changes to the mattress, harness, and incubator system to reduce its resonant frequency and increase damping could potentially decrease RMS WBV by reducing: the hazard weighting at resonance (i.e. W_d and W_k); the degree of resonant driving by vehicle chassis vibration; and the gain at resonance respectively. The air mattress appears promising in this regard; although the air mattress did not significantly decrease WBV, the resonant frequency was reduced to 7Hz, with lower gain at the 14Hz chassis vibration peak. A more compliant mattress system with a peak below 7Hz may result in an overall decrease in vibration exposure, a hypothesis that could be tested experimentally with an underinflated air mattress.

Current transport trolleys use a stiff locking mechanism to clamp directly to the ambulance floor. Although this results in a significant safety improvement in the event of a vehicle accident, vehicle chassis vibration can be transferred directly to the incubator. Hypothetically, an improved coupling incorporating vibration dampening components could dramatically reduce vibration exposure. As the high exposures found in this and several prior studies are potentially an important mechanism of stress and subsequent brain injury associated with inter-hospital transport in babies, it is recommended that development of such designs is pursued as a priority.

Ethics

NHS ethical approval was granted for human volunteer data (Research ethics committee: NRES Committee East Midlands - Nottingham 2, Ref: 12/EM/0257). Study registered with ClinicalTrials.gov (Ref:NCT01851668). Informed consent was obtained in writing from the patient's parents or legal guardian before all neonatal patient transports commenced.

Data accessibility

Data available at `https://datadryad.org/resource/doi:10`

Competing interests

We declare we have no competing interests.

Funding

Acknowledgements

References

[1] Marlow N, Bennett C, Draper E, Hennessy E, Morgan A, Costeloe K. Perinatal outcomes for extremely preterm babies in relation to place of birth in England: the EPICure 2 study. Archives of Disease in Childhood-Fetal and Neonatal Edition. 2014;p. fetalneonatal–2013.

[2] Mohamed MA, Aly H. Transport of premature infants is associated with increased risk for intraventricular haemorrhage. Archives of Disease in Childhood-Fetal and Neonatal Edition. 2010;95(6):F403–F407.

[3] Bowman E, Doyle LW, Murton LJ, Roy R, Kitchen WH. Increased mortality of preterm infants transferred between tertiary perinatal centres. BMJ. 1988;297(6656):1098–1100.

[4] Levene M, Fawer C, Lamont R. Risk factors in the development of intraventricular haemorrhage in the preterm neonate. Archives of disease in childhood. 1982;57(6):410–417.

[5] Shlossman PA, Manley JS, Sciscione AC, Colmorgen G. An analysis of neonatal morbidity and mortality in maternal (in utero) and neonatal transports at 24-34 weeks' gestation. American journal of perinatology. 1997;14(8):449–456.

[6] Shah S, Hudak J, Gad A, Cohen JC, Chander A. Simulated transport alters surfactant homeostasis and causes dose-dependent changes in respiratory function in neonatal Sprague-Dawley rats. Journal of perinatal medicine. 2010;38(5):535–543.

[7] Cochrane DJ, Sartor F, Winwood K, Stannard SR, Narici MV, Rittweger J. A comparison of the physiologic effects of acute whole-body vibration exercise in young and older people. Archives of physical medicine and rehabilitation. 2008;89(5):815–821.

[8] Laksari K, Wu LC, Kurt M, Kuo C, Camarillo DC. Resonance of human brain under head acceleration. Journal of The Royal Society Interface. 2015;12(108):20150331.

[9] Grosek S, Mlakar G, Vidmar I, Ihan A, Primozic J. Heart rate and leukocytes after air and ground transportation in artificially ventilated neonates: a prospective observational study. Intensive care medicine. 2009;35(1):161–165.

[10] Perlman JM, McMenamin JB, Volpe JJ. Fluctuating cerebral blood-flow velocity in respiratory-distress syndrome: relation to the development of intraventricular hemorrhage. New England Journal of Medicine. 1983;309(4):204–209.

[11] ISO 2631-1:1997(E). Mechanical Vibration and Shock-Evaluation of Human Exposure to Whole-Body Vibration. Part I: General Requirements. International Standardisation Organisation, Geneva.; 1997.

[12] Hutchinson, John and Kaiser, Mark J and Lankarani, Hamid M. The head injury criterion (HIC) functional. Applied mathematics and computation. 1998;96(1):1–16.

[13] Eppinger R, Sun E, Bandak F, Haffner M, Khaewpong N, Maltese M, et al. Development of improved injury criteria for the assessment of advanced automotive restraint systems–II. National Highway Traffic Safety Administration. 1999;p. 1–70.

[14] Titterton, David and Weston, John. Strapdown Inertial Navigation Technology (IEE Radar, Sonar, Navigation and Avionics Series). Stevenage: Institution of Electrical Engineers; 1997.

[15] Rimell, Andrew N and Mansfield, Neil J. Design of digital filters for frequency weightings required for risk assessments of workers exposed to vibration. Industrial Health. 2007;45(4):512–519.

[16] Foxlin, Eric. Inertial head-tracker sensor fusion by a complementary separate-bias Kalman filter. In: Virtual Reality Annual International Symposium, 1996., Proceedings of the IEEE 1996. IEEE; 1996. p. 185–194.

[17] WG12, EEVC. 18. Q-dummies Report. Advanced Child Dummies and Injury Criteria for Frontal Impact. EEVC web site; 2008. Available from: http://www.eevc.org/?site=52.

[18] Gajendragadkar G, Boyd J, Potter D, Mellen BG, Hahn G, Shenai JP. Mechanical vibration in neonatal transport: a randomized study of different mattresses. Pediatric Research. 1999;45:198A–198A.

[19] Johannsen H, Trosseille X, Lesire P, Beillas P. Estimating Q-Dummy injury criteria using the CASPER project results and scaling adult reference values. In: Proceedings of IRCOBI Conference, Dublin, Ireland; 2012. .

[20] Griffin M. Minimum health and safety requirements for workers exposed to hand-transmitted vibration and whole-body vibration in the European Union; a review. Occupational and Environmental Medicine. 2004;61(5):387–397.

[21] Campbell AN, Lightstone AD, Smith JM, Kirpalani H, Perlman M. Mechanical vibration and sound levels experienced in neonatal transport. American Journal of Diseases of Children. 1984;138(10):967–970.

[22] Shenai JP, Johnson GE, Varney RV. Mechanical vibration in neonatal transport. Pediatrics. 1981;68(1):55–57.